

Artificial antiphase boundary at the interface of ferrimagnetic spinel bilayers

Ana V. Ramos,¹ Sylvia Matzen,¹ Jean-Baptiste Moussy,¹ Frédéric Ott,² and Michel Viret³

¹CEA-Saclay, IRAMIS, SPCSI, 91191 Gif-Sur-Yvette, France

²CEA-Saclay, IRAMIS, LLB, 91191 Gif-Sur-Yvette, France

³CEA-Saclay, IRAMIS, SPEC, 91191 Gif-Sur-Yvette, France

(Received 24 July 2008; revised manuscript received 12 October 2008; published 5 January 2009)

CoFe₂O₄/Fe₃O₄ bilayers represent an unusual exchange-coupled system whose properties are due to the nature of the oxide-oxide superexchange interactions at the interface. In this work, we analyze the magnetization reversal behavior and magnetic interface structure using a variety of advanced techniques. Low-temperature magnetization, magnetotransport, and polarized neutron reflectivity measurements suggest that the magnetization configuration at the bilayer interface mimics that of an antiphase boundary found in spinel ferrite thin films, thus explaining the unique nature of the magnetic behavior.

DOI: [10.1103/PhysRevB.79.014401](https://doi.org/10.1103/PhysRevB.79.014401)

PACS number(s): 75.70.Cn, 75.60.Jk, 75.10.Pq, 61.05.fj

I. INTRODUCTION

The spinel ferrites have become of great interest to the magnetism community due to their potential applications in spintronic devices. In particular, this family of complex magnetic oxides has been considered for magnetically hard blocking layers,^{1,2} half-metallic electrodes,^{3,4} and most recently for high-temperature spin filters.^{5,6} Another widely studied topic, particularly in the case of Fe₃O₄, is the effect of antiphase boundaries (APBs) on the magnetic^{7,8} and magnetotransport^{9–12} properties. In the present work, we study the magnetic behavior of a particular CoFe₂O₄/Fe₃O₄ bilayer system which could potentially be used in fully epitaxial oxide spin-filter magnetic tunnel junctions (MTJs). CoFe₂O₄ is the magnetic tunnel barrier (or spin filter) and Fe₃O₄ is the magnetic electrode.

This work comes as the sequel to a previous study involving this particular system, in which it was determined that a unique exchange coupling interaction exists between the two ferrimagnets when the thickness of the CoFe₂O₄ layer is reduced to a few nanometers.¹³ Similar exchange interactions have recently been observed in other spinel-spinel bilayer systems.¹⁴ More precisely, we showed that in CoFe₂O₄(5 nm)/Fe₃O₄(15 nm) bilayers, the magnetization reversal occurs in two steps. The CoFe₂O₄ layer reverses first at a magnetic field slightly lower than its usual coercivity, followed by Fe₃O₄ at a magnetic field nearly ten times greater than its intrinsic coercive field. This suggests that there exists a strong exchange interaction between these two layers that is stable in the antiparallel (AP) state—that is, after CoFe₂O₄ has switched. Because of the high Curie temperatures of CoFe₂O₄ and Fe₃O₄ (near 800 K for both), the bilayers correspond to a ferromagnetic-ferromagnetic (FM-FM) exchange-coupled system in all measurements performed at room temperature and below. The goal of this paper is to analyze the nature of the exchange coupling through a series of magnetic and magnetotransport experiments in order to shed light on the nature of the local magnetic configuration at the interface of this unique system.

II. EXPERIMENT

The samples used in the present study were prepared by oxygen plasma-assisted molecular-beam epitaxy (MBE),

as described in Ref. 13. Both Al₂O₃//CoFe₂O₄(5 nm)/Fe₃O₄(15 nm) and Al₂O₃//Fe₃O₄(15 nm)/CoFe₂O₄(5 nm) samples were grown on α -Al₂O₃(0001) substrates, leading to the growth of (111)-oriented spinel films. Their structural and chemical properties were carefully analyzed by a number of standard characterization techniques in order to confirm the composition and fully epitaxial nature of the two layers. Again, the details of the characterization may be found in Ref. 13.

Magnetic measurements of our CoFe₂O₄/Fe₃O₄ bilayers were performed using a vibrating sample magnetometer (VSM) equipped with a cryostat allowing to measure from room temperature down to liquid-helium temperature. Both in-plane and out-of-plane hysteresis loops were measured, revealing a magnetic easy axis in the plane of the films, as expected due to shape anisotropy. The current-in-plane (CIP) magnetotransport characteristics were studied in a Quantum Design physical properties measurement system (PPMS) in a magnetic field of up to ± 7 T. These measurements were performed in the standard four-terminal geometry. Finally, polarized neutron reflectometry (PNR) experiments were performed at the Laboratoire Léon Brillouin facility using polarized neutrons of wavelength $\lambda=4.3$ Å. Spin-up and spin-down (R_{++} and R_{--}) specular reflectivity curves were obtained using the PRISM instrument and these were simulated using least-squares fits with the help of the SIMUL-REFLEC program.¹⁵

III. RESULTS

A. Low-temperature magnetic properties

The original motivation behind the magnetic characterization of the CoFe₂O₄(5 nm)/Fe₃O₄(15 nm) combination was to see if it was possible to obtain an antiparallel magnetic state between the two layers directly in contact with each other, which in turn would permit future tunneling magnetoresistance experiments in Me/CoFe₂O₄/Fe₃O₄-type MTJs, where Me is a nonmagnetic metallic electrode. These particular thicknesses were chosen for two main reasons. First, they are representative of the thicknesses needed for a tunnel barrier/electrode combination. Second, the magnetic proper-

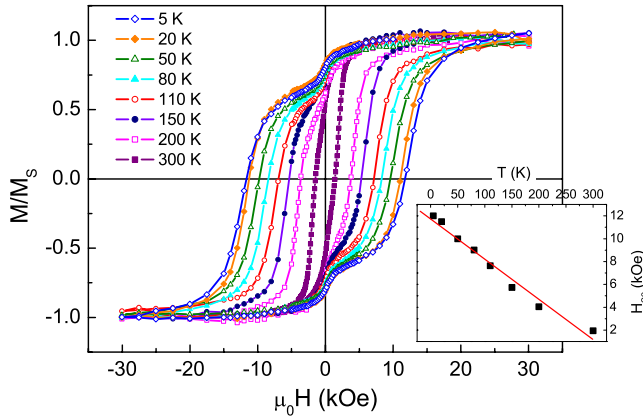


FIG. 1. (Color online) Magnetization curves for a $\text{CoFe}_2\text{O}_4(5 \text{ nm})/\text{Fe}_3\text{O}_4(15 \text{ nm})$ bilayer measured at various temperatures. The normalized hysteresis loops are superposed and reveal a linear evolution of H_{s2} as a function of temperature (inset).

ties of this bilayer system are completely different when the thickness of CoFe_2O_4 is reduced to a few nanometers. While $\text{CoFe}_2\text{O}_4/\text{Fe}_3\text{O}_4$ exchange-coupled systems containing a “thick” (i.e., $>10 \text{ nm}$) CoFe_2O_4 layer have been already studied and reveal typical exchange spring magnet behavior with CoFe_2O_4 playing the role of the hard ferromagnet,^{1,16} none to our knowledge addresses the ultrathin case. Because the coercive field of ultrathin CoFe_2O_4 films is dramatically reduced with respect to thicker films due to the increased presence of antiphase boundaries, we can expect a completely different behavior in this particular system. Our previous magnetization measurements at room temperature revealed magnetization loops displaying two inflection points around 100–160 and 1800–3000 Oe. From now on, these will be labeled H_{s1} and H_{s2} , respectively. Analysis of the magnetization height ratio indicates that $\text{CoFe}_2\text{O}_4(5 \text{ nm})$ is the *first layer* to switch (H_{s1}).¹³ The second inflection point (H_{s2}) therefore corresponds to the switching of the Fe_3O_4 electrode. The virgin in-plane magnetization curves mimic the in-plane hysteresis loop, exhibiting two steps at H_{s1} and H_{s2} which correspond to the switching of CoFe_2O_4 and Fe_3O_4 , respectively. Finally, it is worth noting that the out-of-plane magnetization curves show hysteresis while never reaching the saturation value of the in-plane curve. This behavior is typical of both CoFe_2O_4 and Fe_3O_4 single layers and cannot therefore be associated to the exchange coupling between the two.

In order to further analyze the switching behavior originally observed in our $\text{CoFe}_2\text{O}_4/\text{Fe}_3\text{O}_4$ bilayers, we measured the in-plane magnetization at various temperatures from 300 down to 5 K. The superposition of the magnetization curves is shown in Fig. 1. We observe a systematic accentuation of the two-step magnetization loop with decreasing temperature, with H_{s2} reaching values as high as 1.2 T at 5 K. H_{s1} , on the other hand, remains nearly unchanged. This suggests that the exchange coupling at the interface is so strong that it prevents the coercivity of CoFe_2O_4 from increasing with decreasing temperature, as is commonly observed in uncoupled CoFe_2O_4 single layers.^{17,18} The exchange coupling must therefore favor the early switching of the CoFe_2O_4 layer. Not

only do the low-temperature VSM measurements reinforce the notion that an antiparallel magnetic state is present, but they also reveal the remarkable strength of the exchange interaction at the $\text{CoFe}_2\text{O}_4/\text{Fe}_3\text{O}_4$ interface.

Taking a closer look at the temperature dependence of the $\text{CoFe}_2\text{O}_4(5 \text{ nm})/\text{Fe}_3\text{O}_4(15 \text{ nm})$ $M(H)$ curves, we find that H_{s2} varies linearly with temperature (T) (see the inset of Fig. 1). This evolution is stronger than that observed in both CoFe_2O_4 and Fe_3O_4 single films, thus proving that its origin does not lie in the intrinsic magnetic properties of one of the two layers. Because H_{s2} is related to the magnetic energy of the Fe_3O_4 layer, this means that the sum of the other magnetic energies also displays a linear temperature dependence. These contributions are the magnetocrystalline anisotropies ($K_{\text{CoFe}_2\text{O}_4}$ and $K_{\text{Fe}_3\text{O}_4}$), which are intrinsic to each film, and the exchange energy (E_{ex}) localized at the $\text{CoFe}_2\text{O}_4/\text{Fe}_3\text{O}_4$ interface. It has been shown that $K_{\text{Fe}_3\text{O}_4}$ changes very little with decreasing T and only increases at the Verwey transition,¹⁹ which is absent in our films. $K_{\text{CoFe}_2\text{O}_4}$, on the other hand, has been shown to increase markedly with decreasing T .¹⁷ This suggests that $K_{\text{Fe}_3\text{O}_4}$, although by all means present, plays a much smaller role than $K_{\text{CoFe}_2\text{O}_4}$ in the observed H_{s2} dependence, leaving $K_{\text{CoFe}_2\text{O}_4}$ and E_{ex} to be the principal driving forces. Further theoretical studies would be very useful to clarify the individual contributions of $K_{\text{CoFe}_2\text{O}_4}$ and E_{ex} in the linear evolution of $H_{s2}(T)$.

The shape of the room-temperature and low-temperature $M(H)$ curves suggests that as the magnetic field is lowered from the saturated and “parallel” (P) state past zero field, the CoFe_2O_4 layer switches quite readily. Once in the “antiparallel” state, a strong exchange field between CoFe_2O_4 and Fe_3O_4 stabilizes the system in this configuration, making it extremely difficult for Fe_3O_4 to switch. What is most unique in this system is therefore that the energetically stable or “blocked state” occurs after CoFe_2O_4 has switched, which is rare in exchange-coupled systems involving two ferromagnetic or ferrimagnetic layers. Furthermore, the intrinsic coercivities of the $\text{CoFe}_2\text{O}_4(5 \text{ nm})$ and $\text{Fe}_3\text{O}_4(15 \text{ nm})$ films alone (on the order of 200–300 Oe for both) are so close that it is impossible to predict which of the two layers should act as the “hard” and “soft” ferromagnets. Only when the two are put directly in contact with each other does it finally become clear that CoFe_2O_4 acts as the blocking layer after its own magnetic reversal.

Low-temperature VSM measurements were similarly performed on $\text{Fe}_3\text{O}_4(15 \text{ nm})/\text{CoFe}_2\text{O}_4(5 \text{ nm})$ samples with inverse stacking order. The low-temperature magnetization curves and H_{s2} evolution were comparable to those of the $\text{CoFe}_2\text{O}_4(5 \text{ nm})/\text{Fe}_3\text{O}_4(15 \text{ nm})$ system, confirming that the magnetic behavior of this system is intrinsic to the $\text{CoFe}_2\text{O}_4/\text{Fe}_3\text{O}_4$ interface, regardless of the stacking order.

B. In-plane magnetoresistance measurements

Another method to study the magnetic order (or disorder) in our $\text{CoFe}_2\text{O}_4(5 \text{ nm})/\text{Fe}_3\text{O}_4(15 \text{ nm})$ bilayer samples was to perform CIP transport measurements. This was done by directly placing electrical contacts on the top Fe_3O_4 layer for measurements in the four terminal configurations. Since the

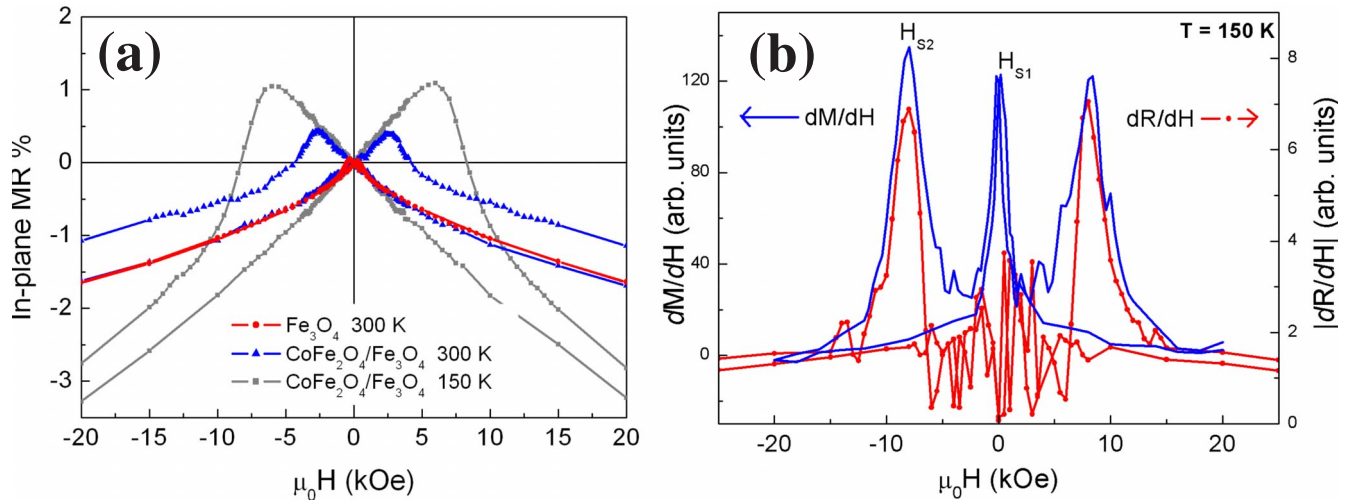


FIG. 2. (Color online) Current-in-plane magnetotransport measurements in a $\text{CoFe}_2\text{O}_4(5 \text{ nm})/\text{Fe}_3\text{O}_4(15 \text{ nm})$ bilayer. (a) Magnetoresistance measurements in the $\text{CoFe}_2\text{O}_4/\text{Fe}_3\text{O}_4$ sample at 300 and at 150 K. The MR curve for a Fe_3O_4 (15 nm) single layer is also shown at 300 K as a reference. (b) Comparison of the derivatives of the magnetization and magnetoresistance curves in a $\text{CoFe}_2\text{O}_4(5 \text{ nm})/\text{Fe}_3\text{O}_4(15 \text{ nm})$ sample at 150 K. dR/dH exhibits one single peak (symmetric for $\pm H$) which aligns perfectly with H_{s2} of dM/dH —that is, with the switching of Fe_3O_4 .

resistivity difference between a 5 nm CoFe_2O_4 layer and a 15 nm Fe_3O_4 film¹² is of the order of 10^3 , we can safely assume that all the current flows in the Fe_3O_4 layer.

The electronic transport in Fe_3O_4 is governed by the FM double exchange interaction between Fe^{2+} and Fe^{3+} cations, which in turn permits electron hopping and thus conduction. When this FM double exchange is disturbed by the presence of defects or other magnetic interactions, the resistance versus applied magnetic-field [$R(H)$] curves in Fe_3O_4 exhibit significant magnetoresistance (MR). Measuring the MR in Fe_3O_4 thin films therefore directly probes the level of magnetic disorder, which in the case of our $\text{CoFe}_2\text{O}_4/\text{Fe}_3\text{O}_4$ system could be influenced by the exchange interactions at the bilayer interface.

One very important point to note about Fe_3O_4 thin films is that these exhibit an intrinsic MR due to the magnetic disorder caused by the presence of APBs.^{9–12} The intrinsic MR at 300 K for a $\text{Fe}_3\text{O}_4(15 \text{ nm})$ single layer grown in our MBE chamber under similar conditions to our $\text{CoFe}_2\text{O}_4/\text{Fe}_3\text{O}_4$ bilayers is shown in red (circles) in Fig. 2(a). In blue (triangles) and in gray (squares) are the MR curves for a $\text{CoFe}_2\text{O}_4(5 \text{ nm})/\text{Fe}_3\text{O}_4(15 \text{ nm})$ bilayer measured at 300 and 150 K, respectively. From these measurements it is quite clear that the MR in Fe_3O_4 is dramatically modified in the bilayer case, indicating that an additional magnetic disorder is created by the interface with CoFe_2O_4 . In other words, the exchange coupling between CoFe_2O_4 and Fe_3O_4 must result in a local magnetic configuration at the interface that significantly disturbs the FM interactions in Fe_3O_4 .

To better interpret the dynamics of magnetic switching behavior, we compared the derivatives of the $R(H)$ and $M(H)$ curves at 150 K. In the case of $M(H)$, the derivative dM/dH exhibits two clear peaks naturally corresponding to the switching events H_{s1} and H_{s2} . On the other hand, the derivative of $R(H)$ contains only one peak which aligns perfectly with that of H_{s2} in dM/dH [see Fig. 2(b)]. This simple

analysis confirms that Fe_3O_4 is the second layer to switch, as was originally deduced from the magnetization height ratio in the $M(H)$ measurements.¹³

The dR/dH characteristics therefore tell us that as the applied magnetic field is lowered from saturation, past the switching of the CoFe_2O_4 layer, the magnetic configuration throughout the entire Fe_3O_4 film does not change significantly. This may be seen by the lack of any noticeable peak in dR/dH from $H=20$ kOe down to $H=H_{s2}$. Only when H becomes great enough to overcome E_{ex} is Fe_3O_4 finally released from the blocked configuration, switching rapidly to realign with the direction of the applied magnetic field. We note that the noise in dR/dH around $-5 \text{ kOe} < \mu_0 H < 5 \text{ kOe}$ is due to a change in the step size in the $R(H)$ measurements and did not result in any reproducible peaks in multiple measurements.

C. Polarized neutron reflectivity

PNR is an extremely valuable tool for the characterization of magnetic multilayers with complex exchange interactions. In the study of our $\gamma\text{-Al}_2\text{O}_3//\text{CoFe}_2\text{O}_4(5 \text{ nm})/\text{Fe}_3\text{O}_4(15 \text{ nm})$ and $\gamma\text{-Al}_2\text{O}_3//\text{Fe}_3\text{O}_4(15 \text{ nm})/\text{CoFe}_2\text{O}_4(5 \text{ nm})$ bilayer systems, PNR provided a complementary analysis of the magnetic reversal behavior to the VSM and PPMS measurements, in particular thanks to its ability to extract magnetization depth profiles across the thickness of the films and at different applied magnetic fields. As was the case with VSM, both stacking orders yielded similar results, again proving that the exchange interaction at the interface was independent of stacking order. For the purposes of this paper, we will therefore focus on the results for the $\gamma\text{-Al}_2\text{O}_3//\text{CoFe}_2\text{O}_4/\text{Fe}_3\text{O}_4$ stacking order only. Following the acquisition of the reflectivity curves, these were fitted by a model that took into consideration the following fitting parameters for each of the

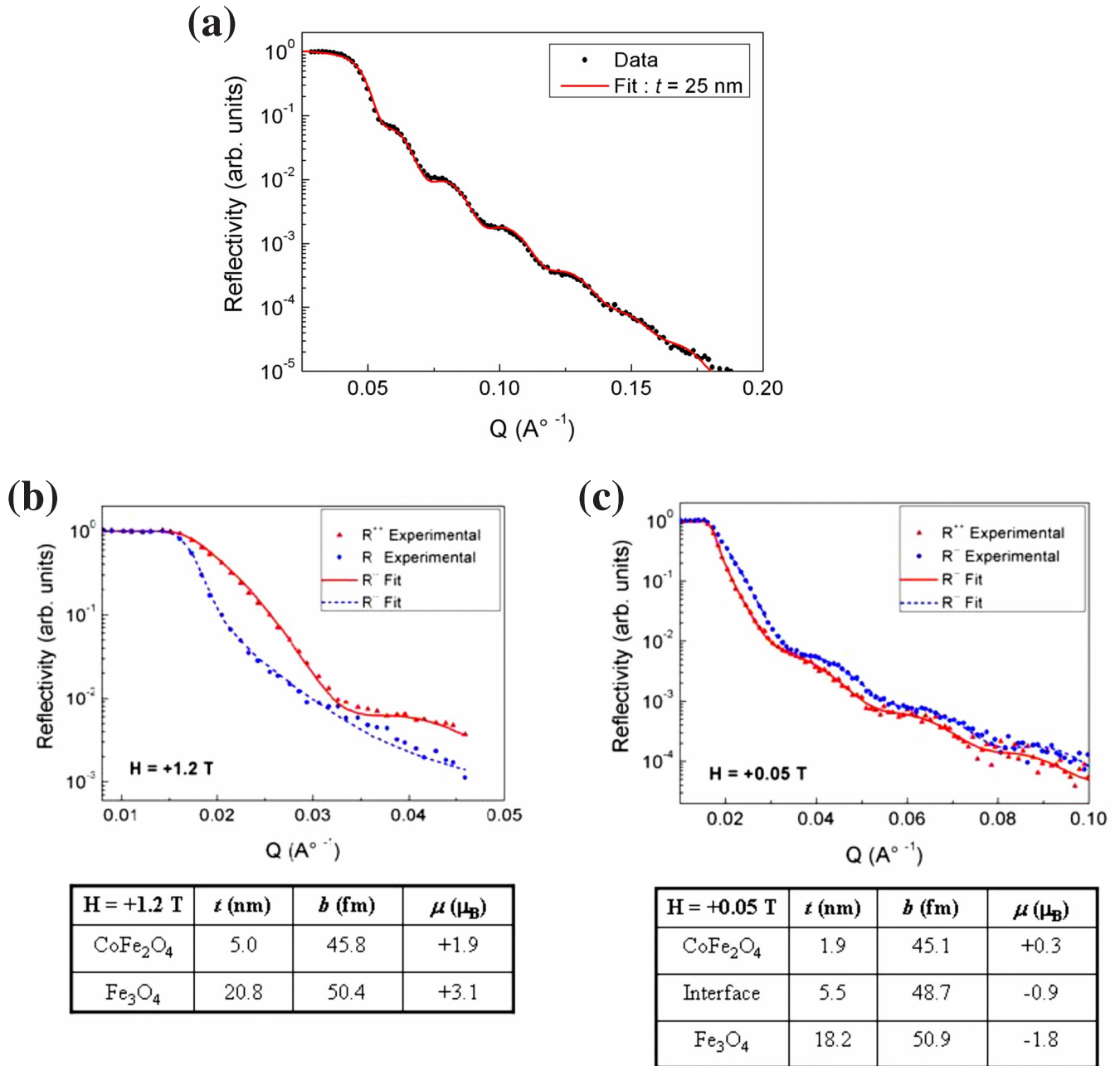


FIG. 3. (Color online) Room-temperature PNR curves for a CoFe₂O₄(5 nm)/Fe₃O₄(15 nm) bilayer at (a) +1.2 T and (b) +0.05 T (coming from negative field $H = -1.2$ T). The tables below each graph show the fitting parameters used to model the experimental curves and thus extract information about the magnetic configuration in the films. The error bar in the measurement of μ is $\pm 0.1\mu_B$.

sample constituents: film thickness (t), material density (ρ in unit cells/m³), neutron-scattering length (b in fm/unit cell), magnetic moment (μ), and roughness (σ). ρ were fixed at 1.36×10^{28} unit cells/m³ for Fe₃O₄ and 1.35×10^{28} unit cells/m³ for CoFe₂O₄ and σ fixed at 0.3 nm for the all of the layers based on x-ray reflectivity measurements. The total thickness of the CoFe₂O₄/Fe₃O₄ bilayer was fixed at 24 ± 1 nm based on x-ray reflectivity measurements as well [see Fig. 3(a)]. The x-ray reflectivity measurements systematically yielded a thickness slightly higher than the aimed 20 nm. The theoretical values for b in CoFe₂O₄ and Fe₃O₄

(44.6 and 51.6 fm, respectively) were used as a guideline for the fits.

PNR measurements on a CoFe₂O₄(5 nm)/Fe₃O₄(15 nm) bilayer deposited directly on α -Al₂O₃ began at the maximum applied magnetic field allowed by the magnet in the neutron spectrometer, which was 1.2 T. At the room-temperature magnetization curve of this sample being closed (i.e., reversible) at 1.2 T, we could assume that our bilayer system was saturated and in the parallel magnetic state. The reflectivity curve and simulation parameters for the CoFe₂O₄(5 nm)/Fe₃O₄(15 nm) bilayer at $H = +1.2$ T and

$T=300$ K are shown in Fig. 3(b). In this figure we see that we are able to reproduce the experimental R_{++} and R_{--} reflectivity curves using a bilayer model in which t , b , and μ of the CoFe_2O_4 and Fe_3O_4 layers correspond well with those expected for 5 and 15 nm films of each material, respectively. This simple PNR measurement confirms the bilayer nature of the sample via a *magnetic* rather than structural or chemical characterization technique.

In the next experiment, we swept the field from $H=-1.2$ T, past the first switching event at H_{s1} , to $H=+0.05$ T. The experimental reflectivity curve obtained at the new field of 0.05 T is shown in Fig. 3(c). This second measurement was only reproducible using a model that contained a magnetization parallel to the applied field for a portion of the CoFe_2O_4 layer, whereas for Fe_3O_4 , the magnetization remained antiparallel to the field. We note that when fitting all of the reflectivity curves at intermediate magnetic fields, the total thickness of the bilayer was fixed to that originally found for the measurement at 1.2 T. This important result confirms the presence of an antiparallel magnetic state for a given magnetic field between H_{s1} and H_{s2} , while also proving that the CoFe_2O_4 film is indeed the first to reverse its magnetization. The negatively magnetized portion of the bilayer had to be broken down into two sublayers of 5.5 and 18.2 nm, the first having a reduced magnetic moment with respect to the second, whereas the thickness of the reversed CoFe_2O_4 layer was determined to be 1.9 nm, thinner than the expected 5 nm. We believe that the second 5.5 nm layer corresponds to an intermediate zone at the $\text{CoFe}_2\text{O}_4/\text{Fe}_3\text{O}_4$ interface that actually includes some of both materials. The reduced moment in this interfacial zone could be explained by the averaged moments of the positive CoFe_2O_4 and negative Fe_3O_4 contributions, as well as by a possible progressive switching of the spins on either side of the interface due to a more complicated local magnetic configuration.

In continuation to the PNR experiment at $H=0.05$ T, we proceeded to trace the magnetization loop past the second switching event at H_{s2} . Seven additional reflectivity curves were obtained, and from them, the corresponding magnetization depth profiles were plotted. These are shown in Fig. 4. We note that the magnetization depicted in these profiles is the projection of the total magnetic moment in the film along \vec{H} , meaning that the reduction in μ may be attributed to a rotation away from the direction of \vec{H} . Since the magnetic domains are very small, no spin-flip signal due to such a helical configuration could be measured. For $H=0.05$, 0.1, and 0.15 T, the magnetization depth profiles display an antiparallel state, in good agreement with the $M(H)$ curve. As the field is increased in this regime, the Fe_3O_4 layer slowly loses some of its magnetic moment, in gradual preparation for the switching event at H_{s2} . CoFe_2O_4 , on the other hand, remains fixed and stable. At $H=0.2$ T, the magnetization of Fe_3O_4 suddenly turns positive, indicating a rapid magnetic reversal at a magnetic field that again agrees well with H_{s2} in the $M(H)$ curve. Finally, for $H=0.25$, 0.3, 0.35, and 1.2 T, we see that once the Fe_3O_4 layer has switched, the two constituents of the bilayer sample rapidly recover their full magnetization and return to the original bilayer configuration depicted in Fig. 3(b).

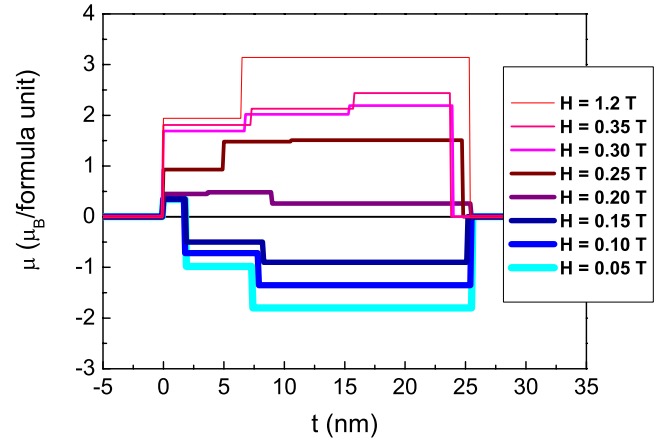


FIG. 4. (Color online) Magnetization depth profiles obtained from room-temperature PNR measurements of the same $\text{CoFe}_2\text{O}_4/\text{Fe}_3\text{O}_4$ sample at different stages of the magnetic hysteresis cycle.

IV. DISCUSSION

The series of VSM and PPMS experiments on the $\text{CoFe}_2\text{O}_4(5 \text{ nm})/\text{Fe}_3\text{O}_4(15 \text{ nm})$ bilayer system reveal a unique magnetization behavior resulting from the nature of the exchange coupling at the interface. The PNR measurements in turn illustrate the step-by-step magnetic reversal process. What makes this system particularly intriguing is that not only are the structure and chemistry of the two films nearly identical but their coercive fields as well. The result is a bilayer system whose magnetization reversal behavior is quite unpredictable. The discussion presented here is meant to analyze the different results presented in the previous experimental sections in order to better understand the coupling mechanism and local magnetic configuration at the interface of our $\text{CoFe}_2\text{O}_4(5 \text{ nm})/\text{Fe}_3\text{O}_4(15 \text{ nm})$ bilayers.

Based on the magnetization curves, CIP magnetotransport measurements, and PNR magnetization depth profiles we have concluded that the CoFe_2O_4 layer switches readily while the Fe_3O_4 layer follows at an unusually large switching field of 1800–3000 Oe (at 300 K). This switching order, which is the opposite of that found in all previous publications involving $\text{CoFe}_2\text{O}_4/\text{Fe}_3\text{O}_4$ exchange-coupled systems, may be explained by the dramatic decrease in coercivity when the CoFe_2O_4 thickness is reduced to a few nanometers. The most probable cause of the decrease in coercive field is the increased presence of APBs in the ultrathin CoFe_2O_4 films, which have been observed experimentally by transmission electron microscopy (not shown). These stacking defects are known to break the magnetocrystalline anisotropy, thus resulting in a significantly reduced coercivity.⁷ It is therefore possible for the CoFe_2O_4 layer to switch before Fe_3O_4 .¹³

In order to illustrate the effect of the magnetocrystalline anisotropy on the switching order in our $\text{CoFe}_2\text{O}_4/\text{Fe}_3\text{O}_4$ bilayers, we analytically calculated the energy in our $\text{CoFe}_2\text{O}_4/\text{Fe}_3\text{O}_4$ bilayers using a one-dimensional model that takes into account only the anisotropy and Zeeman energy terms,

$$E = (K_1 \sin^2 \varphi_1 - HM_1 \cos \varphi_1)t_1 + (K_2 \sin^2 \varphi_2 - HM_2 \cos \varphi_2)t_2, \quad (1)$$

where K is the anisotropy constant, φ is the angle between the magnetization and the applied magnetic field, and t is the film thickness. Here layer 1 is the CoFe_2O_4 and layer 2 is Fe_3O_4 . For the purposes of this calculation, we assumed that $M_1=M_2=350$ kA/m and that $t_1=t_2=15$ nm in order to eliminate the effect of the magnetic mass on the reversal behavior. The decrease in CoFe_2O_4 thickness was therefore represented by a decrease in K_1 , corresponding to the decrease in magnetocrystalline anisotropy caused by APBs. K_2 was held constant at 1.3×10^4 J/m³, which corresponds to the bulk value in Fe_3O_4 .¹⁹ The high K_1 value for CoFe_2O_4 was taken to be 1×10^5 J/m³, which is close to the bulk value.²⁰ Finally K_1 and K_2 are assumed to be in the plane of the film and parallel to H .

The energy profiles were plotted as a function of φ_1 and φ_2 at different applied magnetic fields ranging from +1 to -1 T, allowing us to trace the stable magnetic orientation of each layer and thus the magnetization loop. Figure 5(a) shows the magnetization loops for two bilayer systems: the first with $K_1 > K_2$ and the second with $K_1 < K_2$. We immediately see that only the case $K_1 < K_2$ corresponds to the experimental measurements where $H_{s1} < H_{s2}$ is observed.

In a second calculation, the effect of an exchange interaction at the interface was considered by adding the exchange energy term $A_{\text{AF}}[1 - \cos(\varphi_2 - \varphi_1)]$ to Eq. (1). A_{AF} is the antiferromagnetic exchange constant and is taken to be of the same order as $K \times t \sim 10^{-4}$ J/m². While this is not a physical value, it allows us to study the phenomenological effect of an exchange coupling using the simple analytical model. The resultant magnetization loop for $K_1 < K_2$ is shown in Fig. 5(b). Here we observe that H_{s1} shifts to the right and H_{s2} shifts to the left, while the entire magnetization loop remains centered around zero. This behavior is remarkably similar to what is observed in our experimental magnetization curves. This analytical model is of course largely simplified with respect to the real $\text{CoFe}_2\text{O}_4/\text{Fe}_3\text{O}_4$ system. In particular, it does not take into account the presence of a possible domain wall at the interface, which would require the numerical integration of the exchange energy term across the thickness of both layers, or does it consider the effect of structural defects or magnetic domains on the magnetization reversal behavior. Nevertheless, by simplifying the analysis to one dimension and three parameters, we qualitatively see the effect of the anisotropy and exchange energies on the magnetization reversal behavior, thus allowing us to better analyze exchange coupling at the $\text{CoFe}_2\text{O}_4/\text{Fe}_3\text{O}_4$ interface.

In our previous study of the $\text{CoFe}_2\text{O}_4(5 \text{ nm})/\text{Fe}_3\text{O}_4(15 \text{ nm})$ system, we also discussed the nature of the exchange interaction at the $\text{CoFe}_2\text{O}_4/\text{Fe}_3\text{O}_4$ interface. By analyzing the energies of the different possible exchange interactions in these spinel ferrites, it was concluded that an antiferromagnetic coupling was likely to govern the exchange mechanism at the interface due to its increased stability.¹³ Based on this hypothesis, we should expect a magnetization loop in which the first layer is pushed to switch rapidly leading to an antiparallel configuration that

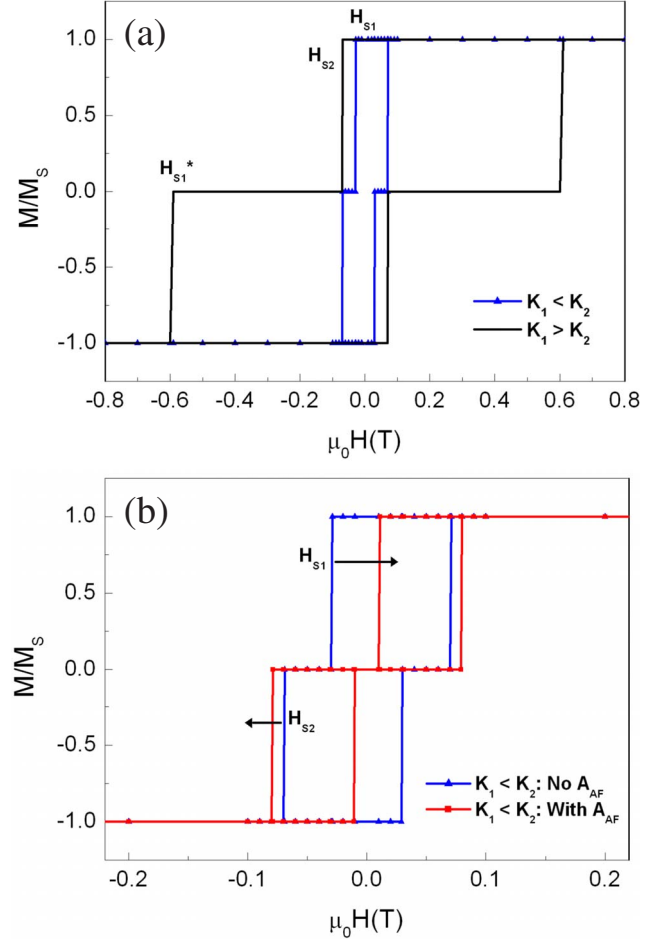


FIG. 5. (Color online) Magnetization loops obtained by using a simple energy model to calculate the magnetic configuration in $\text{CoFe}_2\text{O}_4/\text{Fe}_3\text{O}_4$ bilayers. (a) Effect of the magnetocrystalline anisotropy in CoFe_2O_4 . (b) Effect of an exchange coupling at the $\text{CoFe}_2\text{O}_4/\text{Fe}_3\text{O}_4$ interface in the case of low anisotropy CoFe_2O_4 . H_{s1} and H_{s1}^* are the switching fields for low and high anisotropy CoFe_2O_4 , respectively. H_{s2} corresponds to Fe_3O_4 .

is stabilized by the strong AF exchange field. The strength of the exchange field prevents the second layer from switching immediately, thus leading to an enlarged H_{s2} . Again, this is precisely what is observed in both the low-temperature VSM, PPMS, and PNR measurements, further supporting the original assumption.

Regarding the argument that interdiffusion at the $\text{CoFe}_2\text{O}_4/\text{Fe}_3\text{O}_4$ interface might cause the observed magnetic behavior, we note that both previous chemical studies by transmission electron energy-loss spectroscopy (EELS) (Ref. 13) as well as the present PNR measurements at $H = 1.2$ T unanimously point toward a bilayer structure with an abrupt interface. Furthermore, studies of the magnetic properties of substoichiometric $\text{Co}_{(1-x)}\text{Fe}_{(2+x)}\text{O}_4$ single layers show that the coercivity gradually decreases with decreasing Co content.²¹ The abrupt two-phase nature of the bilayer hysteresis loops does not agree with this gradual evolution. We therefore exclude interdiffusion as a possible explanation for the observed magnetic behavior.

After understanding the nature of the coupling and the general magnetization reversal mechanism in our

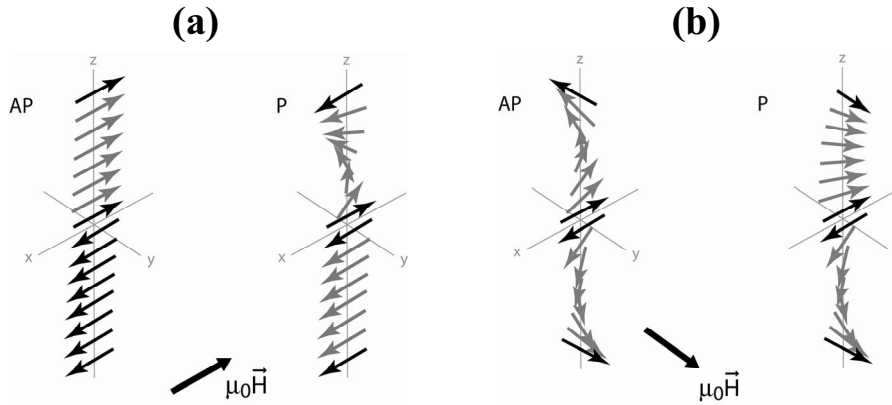


FIG. 6. Schematic illustration of two possible scenarios for the alignment of an AF coupling at the $\text{CoFe}_2\text{O}_4/\text{Fe}_3\text{O}_4$ interface with respect to an applied magnetic field: (a) coupling parallel to \vec{H} ; (b) coupling perpendicular to \vec{H} . In both cases, the expected local magnetic configuration involves the formation of a domain wall on one or both sides of the interface in order to recover a P or AP state far from the interface.

$\text{CoFe}_2\text{O}_4(5 \text{ nm})/\text{Fe}_3\text{O}_4(15 \text{ nm})$, the next step is to define the local magnetic configuration at the bilayer interface. Here the interpretation becomes more delicate as none of the experimental methods described above give direct access to this information. To begin, we observe that there is a positive slope in the magnetization curve with respect to the applied field in the range between H_{s1} and H_{s2} both at room temperature and at low temperature (Fig. 1). The positive slope is also visible in the tail of CoFe_2O_4 minor loops previously shown in Ref. 13. This detail leads us to believe that a domain wall is present at the interface for this field range. In fact, such a slope has been previously determined to correspond to the compression of an interfacial domain wall present in FM/FM exchanged-coupled interfaces.²² In the case of our $\text{CoFe}_2\text{O}_4(5 \text{ nm})/\text{Fe}_3\text{O}_4(15 \text{ nm})$ bilayers, this would suggest that there exists a progressive rotation of the spins, coupled antiferromagnetically on either side of the interface, toward a parallel or antiparallel alignment (depending on the magnitude of the applied magnetic field) far from the interface.

The possibility of an interfacial region containing a domain-wall structure is further supported by the magnetization depth profiles in the PNR measurements. In Fig. 4, we see that all of the profiles obtained in the AP configuration contain an interfacial region of a few nanometers in thickness, covering part of CoFe_2O_4 and part of Fe_3O_4 , with a reduced magnetization with respect to Fe_3O_4 . As was mentioned earlier, this interfacial layer of the depth profile could be due to a progressive switching of the antiparallel moments in CoFe_2O_4 toward the parallel moments in Fe_3O_4 . The reduced negative moment would therefore correspond to the average of the moments in both layers projected along the direction of the applied field across the entire thickness of this interfacial domain wall. In order to better identify the structure at the interface, the PNR curves could have been fitted with a greater number of sublayers at the $\text{CoFe}_2\text{O}_4/\text{Fe}_3\text{O}_4$ interface. However, doing so would introduce a significant number of additional variables into the model and thus considerably reduce the reliability of the fits. We have therefore chosen to rely on the three sublayer model depicted in Fig. 4.

Assuming that the AF coupling at the $\text{CoFe}_2\text{O}_4/\text{Fe}_3\text{O}_4$ interface is associated to a domain wall on one or both sides and that this AF coupling appears as soon as the bilayer is deposited, there are two possible scenarios for the orientation of an AF coupling with respect to the applied magnetic field: an AF coupling parallel to H or an AF coupling *perpendicular* to H [Figs. 6(a) and 6(b), respectively]. The first scenario leads to a domain wall only in the P state, predominant in one of the two films, whereas in the latter case, the domain wall exists both in the P and AP states and traverses both layers. Based on a simple energy minimization calculation of two AF-coupled spins in a planar applied field, the most favorable configuration is a coupling that is oriented perpendicular to the magnetic field and also in the plane of the films. The structure is schematically illustrated in Fig. 6 for both the P and AP states. The progressive rotation of the spins on either side of the AF coupling, also referred to as two AF-coupled half spin chains, agrees well with the hypothesis that a domain wall forms at the $\text{CoFe}_2\text{O}_4/\text{Fe}_3\text{O}_4$ interface and spans across both layers.

Furthermore, the magnetization reversal behavior associated with Fig. 6(b) also corresponds very well with the results obtained in the magnetotransport measurements. Because the AF coupling at the interface is oriented perpendicular to H , the spins in the CoFe_2O_4 layer may rotate freely from P to AP at H_{s1} , without affecting the AF coupling at the interface or the magnetic order in Fe_3O_4 . We recall that the MR properties of Fe_3O_4 suggested that this layer maintains the same magnetic configuration starting from the P state at saturation all the way through the switching of CoFe_2O_4 at H_{s1} . This magnetic configuration is different than that in a free layer since the MR curve is significantly modified, again supporting the existence of part of the domain wall in Fe_3O_4 . The MR characteristics only indicate a significant change in magnetic order (or better, disorder) when the applied field reaches H_{s2} , as one would expect given the configuration depicted in Fig. 6(b).

The presence of a domain-wall structure consisting of two half spin chains coupled antiferromagnetically at an angle of 90° with respect to the applied field is precisely the local magnetic structure associated with antiphase boundaries

commonly found in spinel ferrite films.^{7,11,12,23} In certain APBs, the stacking fault generates an additional AF coupling that is oriented perpendicular to the applied field. Far from the APB, the spins realign along H , and this is achieved via a progressive rotation of the spins on either side of the APB toward the P configuration, exactly as is shown in the P scenario in Fig. 6(b). In other words, the local magnetic configuration that we predict at the $\text{CoFe}_2\text{O}_4/\text{Fe}_3\text{O}_4$ interface when the bilayer system is in the P or saturated state is in essence an “artificial APB.” In the AP state, the configuration corresponds to an APB in which the two half spin chains rotate in opposite directions. We therefore believe that the structural and magnetic defect generated by the $\text{CoFe}_2\text{O}_4/\text{Fe}_3\text{O}_4$ interface is, in fact, equivalent to a special type of APB in which the two AF-coupled half spin chains may switch from P to AP depending on the magnitude and direction of the external magnetic field.

It is important to mention that the local magnetic configuration proposed in this discussion is surely simplified with respect to reality. In particular, we know that our $\text{CoFe}_2\text{O}_4(5\text{ nm})/\text{Fe}_3\text{O}_4(15\text{ nm})$ bilayers contain many small magnetic domains generated by the presence of APBs in the films. These domains, having a size on the order of 100 nm, inevitably influence the overall switching behavior in our system. The AF-coupled spin-chain configuration proposed above is therefore probably repeated from one domain to another, leading to a situation that is more complex than that described above. Whether or not these domains act independently of each other is a question that for the moment remains unanswered. Also, we do not know to what extent the boundary conditions imposed by the small domain size affect the spin-chain configuration in each domain. Further

numerical simulations of a multidomain system in which each domain contains an artificial APB like that described above should improve the understanding of this complex problem.

V. CONCLUSION

In conclusion, the magnetic switching behavior of fully epitaxial $\text{CoFe}_2\text{O}_4(5\text{ nm})/\text{Fe}_3\text{O}_4(15\text{ nm})$ bilayers has been studied using VSM, CIP magnetotransport measurements, and PNR. We have shown that by directly growing Fe_3O_4 on CoFe_2O_4 or vice versa, a two-phase magnetization loop may be obtained without the insertion of a nonmagnetic spacer. This magnetization loop reveals a strong exchange coupling interaction between the two layers that blocks the Fe_3O_4 layer in the antiparallel state, after CoFe_2O_4 has switched. Careful analysis of the magnetic and magnetotransport measurements suggests that the local magnetic configuration at the $\text{CoFe}_2\text{O}_4/\text{Fe}_3\text{O}_4$ interface involves a domain-wall-type structure containing two AF-coupled half spin chains, thus generating an artificial antiphase boundary. The unique magnetic properties of this bilayer system therefore make it an interesting candidate for future theoretical studies, as well as spin-polarized transport measurements in spin-filter MTJs.

ACKNOWLEDGMENTS

The authors would like to thank M. Gautier-Soyer for the useful discussions. We are also very grateful to P. Bonville for the help with the low-temperature VSM experiments. This project was partially funded by the CNANO Île de France “FILASPIN” project.

-
- ¹Y. Suzuki, R. B. van Dover, E. M. Gyorgy, J. M. Phillips, and R. J. Felder, *Phys. Rev. B* **53**, 14016 (1996).
- ²N. Viart, R. Sayed Hassam, C. Mény, P. Panissod, C. Ulhaq-Bouillet, J. L. Loison, G. Versini, F. Huber, and G. Pourroy, *Appl. Phys. Lett.* **86**, 192514 (2005).
- ³P. Seneor, A. Fert, J.-L. Maurice, F. Petroff, and A. Vaures, *Appl. Phys. Lett.* **74**, 4017 (1999).
- ⁴G. Hu and Y. Suzuki, *Phys. Rev. Lett.* **89**, 276601 (2002).
- ⁵U. Luders, M. Bibes, K. Bouzehouane, E. Jacquet, J.-P. Contour, S. Fusil, J. Fontcuberta, A. Barthélémy, and A. Fert, *Appl. Phys. Lett.* **88**, 082505 (2006).
- ⁶A. V. Ramos, M.-J. Guittet, J.-B. Moussy, R. Mattana, C. Deranlot, F. Petroff, and C. Gatel, *Appl. Phys. Lett.* **91**, 122107 (2007).
- ⁷D. T. Margulies, F. T. Parker, M. L. Rudee, F. E. Spada, J. N. Chapman, P. R. Aitchison, and A. E. Berkowitz, *Phys. Rev. Lett.* **79**, 5162 (1997).
- ⁸J.-B. Moussy, S. Gota, A. Bataille, M.-J. Guittet, M. G. Soyer, F. Delille, B. Dieny, F. Ott, T. D. Doan *et al.*, *Phys. Rev. B* **70**, 174448 (2004).
- ⁹J. M. D. Coey, A. E. Berkowitz, L. Balcells, F. F. Putris, and F. T. Parker, *Appl. Phys. Lett.* **72**, 734 (1998).
- ¹⁰M. Ziese and H. J. Blythe, *J. Phys.: Condens. Matter* **12**, 13 (2000).
- ¹¹W. Eerenstein, T. T. M. Palstra, S. S. Saxena, and T. Hibma, *Phys. Rev. Lett.* **88**, 247204 (2002).
- ¹²A. V. Ramos, J. B. Moussy, M. J. Guittet, A. M. Bataille, M. Gautier-Soyer, M. Viret, C. Gatel, P. Bayle-Guillemaud, and E. Snoeck, *J. Appl. Phys.* **100**, 103902 (2006).
- ¹³A. V. Ramos, J.-B. Moussy, M.-J. Guittet, M. Gautier-Soyer, C. Gatel, P. Bayle-Guillemaud, B. Warot-Fonrose, and E. Snoeck, *Phys. Rev. B* **75**, 224421 (2007).
- ¹⁴B. B. Nelson-Cheeseman, R. V. Chopdekar, J. S. Bettinger, E. Arenholz, and Y. Suzuki, *J. Appl. Phys.* **103**, 07B524 (2008).
- ¹⁵<http://www.llb.cea.fr/prism/programs/simulreflec/simulreflec.html>
- ¹⁶M. Ziese, R. Hohne, A. Bollero, H. C. Semmelhack, P. Esquinazi, and K. Zimmer, *Eur. Phys. J. B* **45**, 38054 (2005).
- ¹⁷L. Horng, G. Chern, M. C. Chen, P. C. Kang, and D. S. Lee, *J. Magn. Magn. Mater.* **270**, 389 (2004).
- ¹⁸C. Gatel, Ph.D. thesis, INSA Toulouse, 2004.
- ¹⁹L. R. Bickford, *Phys. Rev.* **76**, 137 (1949).
- ²⁰Y. Suzuki, G. Hu, R. B. van Dover, and R. J. Cava, *J. Magn. Magn. Mater.* **191**, 1 (1999).
- ²¹A. V. Ramos (unpublished).
- ²²F. Canet, C. Bellouard, L. Joly, and S. Mangin, *Phys. Rev. B* **69**, 094402 (2004).
- ²³H. Zijlstra, *IEEE Trans. Magn.* **15**, 1246 (1979).